DYNAMICAL EMISSION AND ISOTOPE THERMOMETRY

H.F. Xi, G.J.Kunde[a], O. Bjarki, C.K. Gelbke, R.C. Lemmon[b], W.G. Lynch, D. Magestro, R. Popescu[c], R.Shomin, M.B. Tsang, A.M. Vander Molen, G.D. Westfall G. Imme[d], V. Maddalena, C. Nociforo[d], G. Raciti[d], G. Riccobene[d], F.P. Romano[d], A. Saija[d], C. Sfienti[d], S.Fritz[e], C. Gross[e], T. Odeh[e], C. Schwarz[e], A. Nadasen[f], D. Sisan[f], K.A.G. Rao[f]

Temperatures for hot nuclear systems formed in nucleus-nucleus collisions have been extracted from the comparison of ratios of isotopic yields, T_{iso} [1-7], and excited state populations, $T_{\Delta E}$ [4, 7, 9-12]. For thermal distributions at low density and at chemical equilibrium, prior to the secondary decay of the excited fragments, the double ratios R_{iso} of the ground state yields of four suitably chosen isotopes are given by [1]:

$$R_{iso} = \frac{Y(A_1,Z_1)/Y(A_1+1,Z_1)}{Y(A_2,Z_2)/Y(A_2+1,Z_2)} = \frac{1}{a} exp(B/T) \qquad (1)$$

where $Y(A_i, Z_i)$ is the yield for isotope with mass A_i and charge Z_i; a is a statistical factor determined by spin values and kinematics factors; $B = BE(A_1,Z_1) - BE(A_1+1,Z_1) - BE(A_2,Z_2) + BE(A_2+1,Z_2)$; and $BE(A_i,Z_i)$ is the binding energy of the i^{th} nucleus

Similarly, the ratios R_{ij} of the yields of states i and j of a specific fragment, prior to the secondary decay of the excited fragments, are given by [8]:

$$R_{ij} = \frac{Y_i}{Y_j} = \frac{(2J_i+1)}{(2J_j+1)} e^{-(E_i^* - E_j^*)/T} \qquad (2)$$

Where Y_i is the yield, E_i^* is the excitation energy, and J_i is the spin of the state i.

The experiment was performed by bombarding ^{93}Nb targets of 6 and 20 mg/cm^2 areal density with ^{86}Kr beams at E/A=35, 70, 100, 120 MeV from the National Superconducting Cyclotron Laboratory at Michigan State University (MSU). Impact parameters were selected by gates on the multiplicity of identified charged particles detected at polar angles of θ_{lab} = 7°-157° using 215 plastic ΔE-E phoswich detectors of the MSU 4π Array. The data presented here represent central collisions with a charged particle multiplicity selection on the MSU 4π array corresponding to the top 20% of the total cross section and reduced impact parameter $b/b_{max} \leq 0.45$.

The relative populations of widely separated states in emitted 4He ($J_i^\pi = 0^+, E^* = 20.1$ MeV; $J_j^\pi = 0^+$, g.s.), 5Li ($J_i^\pi = 3/2^+, E^* = 16.7$ MeV; $J_j^\pi = 3/2^-$, g.s.), and 8Be ($J_i^\pi = 1^+, E^* = 17.6$ MeV; $J_j^\pi = 2^+, E^* = 3$ MeV) fragments were measured with the 96 element hodoscope.

Correlation functions, $R(E_{rel})$, which are defined in terms of the measured coincidence yield $Y_{12}(p_1, p_2)$ and the singles yield $Y_1(p_1)$ and $Y_2(p_2)$ as follows:

$$\Sigma Y_{12}(p_1, p_2) = C[1 + R(E_{rel})] \Sigma Y_1(p_1) Y_2(p_2). \qquad (3)$$

Here, p_1 and p_2 are the momenta of the two particles in the laboratory and $E_{rel} = \frac{1}{2}\mu v_{rel}^2$ is the kinetic energy in the center-of-mass frame of the two particles. The sums on both sides of Eq. (3) are extended over all energy, position and detector combinations corresponding to a given bin of E_{rel}. The normalization constant C in Eq. (3) is chosen to normalize $1 + R(E_{rel})$ to unity at large E_{rel} where resonances are not observed in the exit channel.

The solid points in Fig. 1 correspond to the correlation functions measured using the previously described central collision gate. The d-^{3}He correlation function in the upper panel of the figure displays

a structure at low E_{rel} corresponding to the J^{π} = 3/2^{+} E^{*} = 16.7 MeV excited state and the p-α correlation in the lower panel displays a broad structure at $E_{rel} \approx 2$ MeV corresponding to J^{π} = 3/2^{-} ground state of ^{5}Li. The coincidence yield in the correlation function was fitted by superimposing the resonant decay of ^{5}Li and a non-resonant contribution wherein the two measured coincident particles are emitted independently but interact by long range mutual Coulomb interactions as they propagate from the production region. The response of the experimental apparatus was folded into the calculations. The solid, dashed and dotted lines represent minimum and maximum background estimates from different assumption on the uncorrelated emission evaluated by model calculations. Both the full fit and the corresponding non-resonant background are separately shown.

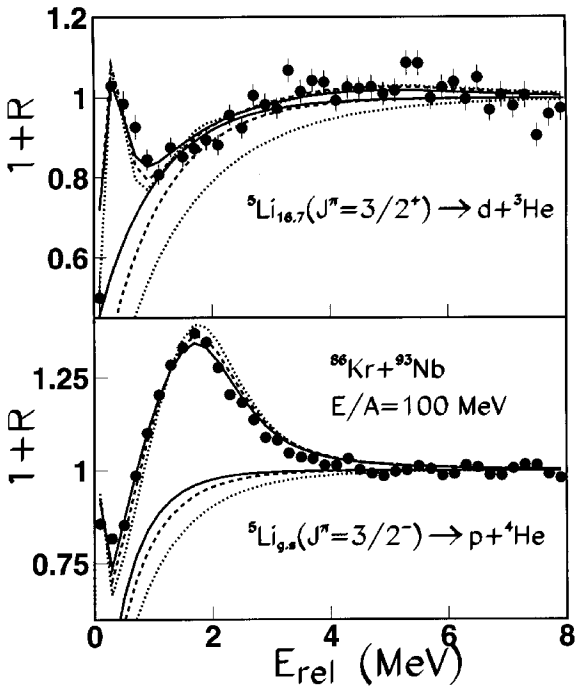

Fig. 1: Correlation functions, exhibiting the decay of ^{5}Li in its E*=16.7 MeV excited state (top panel) and its ground state (bottom panel), as a function of relative energy of the decay products.

Extracted values of $T_{\Delta E}$ are plotted as solid circles ($T_{\Delta E}$ (^{5}Li)), solid diamonds ($T_{\Delta E}$ (^{4}He)), and solid squares ($T_{\Delta E}$ (^{8}Be)) in Figure 2 as a function of incident energy. The experimental uncertainties primarily reflect uncertainties in the subtraction of the non-resonant background. The extracted temperatures $T_{\Delta E}$ are of the order of 4 MeV and show little variation with incident energy, a trend also observed for central Au + Au collisions [4,7].

Values of T_{iso} were obtained via Eq. (1) at the four incident energies. Carbon isotope yields were measured with the heavy-ion telescopes while the isotope yield ratios for lighter particles (Z<6) were obtained with selected detectors in the hodoscope situated at $\theta_{cm} \approx 90° \pm 10°$. (Over the measured angular range, all the single isotope yield ratios are relatively constant with respect to scattering angle.) The experimental uncertainties in these ratios mainly reflected the uncertainties in the particle identification (up to 10% in ^{11}C). Values for T_{iso}*(C-Li)* (open circles) obtained from (^{6,7}Li, ^{11,12}C) isotope ratios vary little with incident energy, similar to the trends exhibited by the temperatures $T_{\Delta E}$ (^{5}Li), $T_{\Delta E}$ (^{4}He), and $T_{\Delta E}$ (^{8}Be) extracted from excited states populations. In contrast, values of T_{iso}*(He-Li)* (open diamonds) obtained from (^{6,7}Li, ^{3,4}He) isotopes increase monotonically with incident or excitation energy, consistent

with trends recently reported for other systems [7]. Similarly increasing trends are extracted from other possible ratios based upon the large binding energy difference between ^{3}He and ^{4}He isotopes.

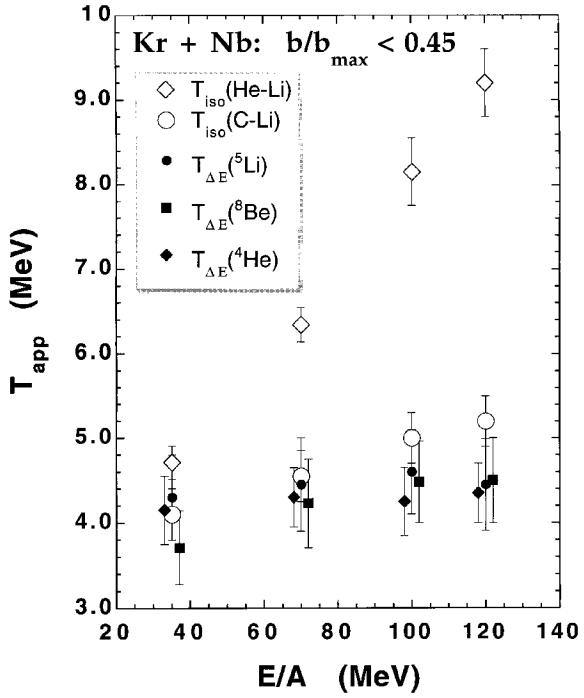

Fig. 2: Dependence of T_{iso} (open symbols) and $T_{\Delta E}$ (closed symbols) upon the incident energy.

The overall picture provided by the present data suggests that the temperatures deduced from the ^{3}He yields are inconsistent with all other cases investigated for which $B >> T$. This discrepancy may reflect differences in the emission environments of ^{3}He as compared to the emission environments for fragments and alpha particles. Theoretical support for this picture is provided by the predictions of dynamic models for light particle emission and also by statistical emission rate approaches [13, 14]. The precise degree to which light particle emission during the early stages of the collision is further enhanced by statistical emission of predominantly light particles at very high initial temperature depends on the timescale for thermalization and requires further experimental and theoretical investigations. Qualitatively, however, both effects will cause a divergence of temperatures derived from poorly bound light particles such as d, t, ^{3}He from those derived from strongly bound fragments observed in the present work.

a: Present address: Yale University, New Haven CT 06520, U.S.A
b: Present address: CCLRC, Daresbury Laboratory, Daresbury, Cheshire, WA44AD, U.K
c: Present address: Brookhaven National Laboratory, Upton, NY11973, U.S.A
d: Dipartimento di Fisica Universita and I>N>F>N Sezione and Laboratorio Nazionale del SUD – Catania, I95127, Catania, Italy
e: Gesellschaft fur Schwerionenforschung, D-64220 Darmstadt, Germany
f: Department of Natural Sciences, University of Michigan, Dearborn, Mi48128, USA

References:

1. S. Albergo et al., Nuovo Cimento **89**, 1 (1985).
2. J. Pochodzalla et al., Phys. Rev. Lett. **75**, 1040 (1995).
3. M.B. Tsang, W.G. Lynch, H. Xi, W.A. Friedman, Phys. Rev. Lett. **78**, 3836 (1997).
4. M.J. Huang et. al., Phys. Rev. Lett. **78**, 1648 (1997).
5. R. Wada et al., Phys. Rev. **C 55**, 227 (1997).
6. Y-G. Ma et. al, Phys. Lett. B, **B390**, 41 (1997).
7. V. Serfling et al., GSI preprint, GSI98-06 (1998).
8. W. Benenson, D. J. Morrissey, and W. A. Friedman, Ann. Rev. Nucl. and Part. Sci. **44**, 27 (1994), and refs. therein.
9. T.K. Nayak et al., Phys. Rev. **C 45**, 132 (1992).
10. F. Zhu et al., Phys. Rev. **C 52**, 784 (1995).
11. J. Pochodzalla et al., Phys. Rev. **C35**, 1695 (1987).
    Z. Chen et al., Phys. Rev. **C36**, 2297 (1987).
12. C. Schwarz et. al. Phys. Rev. **C 48**, 676 (1993).
13. R. Bougault et al., preprint, LPCC97-04 (1997).
14. H. Xi et al., Phys. Rev. C, Phys. Rev. **C 57**, R467 (1998).